

## MATCHED ASYMPTOTIC EXPANSIONS FOR FREE CONVECTION ABOUT AN IMPERMEABLE HORIZONTAL SURFACE IN A POROUS MEDIUM

I. D. CHANG

Department of Aeronautics and Astronautics, Stanford University, Stanford, CA 94305, U.S.A.

and

P. CHENG

Department of Mechanical Engineering, University of Hawaii at Manoa, Honolulu, HI 96822, U.S.A.

(Received 12 April 1982 and in final form 24 June 1982)

**Abstract**—The problem of steady free convection in a porous medium adjacent to a horizontal impermeable heated surface, with wall temperature distribution  $\hat{T}_w = \hat{T}_\infty + Ax^\lambda (0 \leq \lambda < 2)$ , for  $\hat{x} \geq 0$  and  $\hat{T} = \hat{T}_\infty$  for  $\hat{x} < 0$ , is investigated by the method of matched asymptotic expansions. The small parameter in the perturbation series is found to be the inverse one-third power of the Rayleigh number. For the first-order inner problem the governing equations reduced to the boundary layer approximations which have been solved previously. The effects of fluid entrainment, streamwise heat conduction and upward-drift induced friction are taken into consideration in the second and third-order theory for which similarity solutions are obtained. Numerical results for temperature and streamwise velocity profiles as well as the local Nusselt number at different local Rayleigh numbers and different prescribed wall temperature distributions are presented. It was found that the local Nusselt numbers as obtained from the boundary layer theory for  $\lambda = 0.5$  are accurate to the third-order, while those for  $\lambda = 0$  are accurate to the second-order. For other values of  $\lambda$ , the boundary layer theory underestimates the local Nusselt number slightly; the accuracy of the boundary layer theory decreases as the Rayleigh numbers decrease and as  $\lambda$  increases from  $\lambda = 0.5$ .

### NOMENCLATURE

$A$ ,	constant defined in equation (4b);	$v$ ,	dimensionless Darcian velocity in the y-direction;
$A_1, A_2, \dots$ ,	constants defined in equation (87a);	$X$ ,	dimensionless inner coordinate;
$B_1, B_2, \dots$ ,	constants defined in equation (87b);	$x$ ,	dimensionless coordinate;
$C$ ,	constant defined in equation (56b);	$Y$ ,	dimensionless inner coordinate;
$c$ ,	constant defined in equation (49);	$y$ ,	dimensionless coordinate.
$c_1, c_2, \dots$ ,	constants defined in equation (37b);	Greek symbols	
$D$ ,	constant defined in equation (51a);	$\alpha$ ,	equivalent thermal diffusivity;
$f_0, f_1, \dots$ ,	dimensionless perturbation stream functions;	$\alpha_m$ ,	exponent of the perturbation parameter;
$g$ ,	acceleration due to gravity;	$\beta$ ,	coefficient of thermal expansion;
$g_0, g_1, \dots$ ,	dimensionless perturbation temperature functions;	$\Gamma$ ,	exponent defined in equation (78);
$h$ ,	local heat transfer coefficient;	$\gamma$ ,	exponent defined in equation (37);
$K$ ,	permeability of the porous medium;	$\varepsilon$ ,	perturbation parameter;
$k$ ,	thermal conductivity of the porous medium;	$\eta$ ,	similarity variable;
$L$ ,	a characteristic length;	$\Theta$ ,	dimensionless inner temperature;
$m$ ,	constant defined in equation (49);	$\theta$ ,	dimensionless temperature;
$Nu_x$ ,	local Nusselt number;	$\Lambda$ ,	constant defined in equation (49);
$p$ ,	pressure;	$\lambda$ ,	constant defined in equation (4b);
$q$ ,	local heat transfer rate;	$\rho$ ,	density of the fluid;
$r$ ,	radial distance from the origin;	$\sigma$ ,	constant defined in equation (77);
$Ra_x$ ,	local Rayleigh number;	$\mu$ ,	viscosity of the fluid;
$T$ ,	dimensionless temperature;	$\Psi$ ,	dimensionless inner stream function;
$U$ ,	dimensionless inner variable for Darcian velocity in the x-direction;	$\psi$ ,	dimensionless stream function.
$u$ ,	dimensionless Darcian velocity in the x-direction;	Superscript	
$V$ ,	dimensionless inner variable for Darcian velocity in the y-direction;	,	dimensionless variables defined in equation (70).
		Subscripts	
		$\infty$ ,	condition at infinity;
		$w$ ,	condition at the wall.

## 1. INTRODUCTION

THE PREDICTION of convective heat transfer from a heated impermeable surface in a saturated porous medium has important applications in the assessment of geothermal resources and the design of underground energy storage systems. In a recent paper, Cheng and Chang [1] obtained a similarity solution for steady free convection in a porous medium adjacent to a heated or cooled horizontal surface on the basis of the boundary layer approximations. The analysis neglects the streamwise heat conduction and the upward-drift induced friction within the boundary layer. In addition, no account is taken of interactions, such as fluid entrainment between the outer region and the boundary layer. The boundary layer approximations are valid mathematically if the value of the Rayleigh number approaches infinity. For most of the convective heat transfer problems in a sub-surface formation, however, the values of the Rayleigh number are not very large and the thermal boundary layers are relatively thick. Thus, for most practical applications, it would be of great interest to refine the boundary layer analysis to include the higher-order effects so that results can be applicable to smaller values of the Rayleigh number.

In the classical viscous flow theory, refinements to the boundary layer analysis for many problems have been obtained by the method of matched asymptotic expansions [2]. For problems of free convection about an isothermal plate in a viscous fluid, higher-order approximations based on matched asymptotic expansions have been obtained by a number of investigators [3–7]. In particular, a higher-order approximation for free convection about a horizontal plate in a viscous fluid has been obtained by Mahajan and Gebhart [6].

In this paper, we shall use the method of matched asymptotic expansions to study the higher-order effects for the problem of free convection in a Darcian fluid adjacent to a horizontal heated impermeable surface with temperature given by  $\hat{T}_w = \hat{T}_\infty + A\hat{x}^\lambda$  (with  $A > 0$  and  $0 \leq \lambda < 2$ ) for  $\hat{x} \geq 0$  and  $\hat{T}_w = \hat{T}_\infty$  for  $\hat{x} < 0$ , where  $\hat{x}$  is the coordinate along the bounding surface with the  $y$ -coordinate perpendicular to the surface and pointing toward the porous medium with temperature  $\hat{T}_\infty$  at  $\hat{y} \rightarrow \infty$ . The purpose of this paper is to extend the applicability of the boundary layer theory to lower Rayleigh number ranges. In the following it will be shown that the perturbation equation for free convection in a porous medium adjacent to a heated horizontal surface is a singular one at large Rayleigh numbers. For the first-order inner problem the governing equations will be shown to be identical to the boundary layer approximations which have been solved previously [1]. Similarity solutions will be obtained for the second and third-order inner problems. Numerical results for temperature and streamwise velocity profiles as well as the local Nusselt number at different local Rayleigh numbers and different prescribed wall temperature distributions will be presented. For the case of an isothermal wall ( $\lambda = 0$ ),

it was found that the local Nusselt numbers as obtained from the boundary layer theory are accurate to the second-order, while those for the case of constant surface heat flux ( $\lambda = 0.5$ ), are accurate to the third-order. For other values of  $\lambda$ , it was found that the boundary layer theory underestimates the local Nusselt number. The accuracy of the boundary layer theory decreases as  $\lambda$  is increased from  $\lambda = 0.5$ .

## 2. ANALYSIS

If we assume that (i) the convective fluid and the porous medium are in local thermal equilibrium, (ii) the properties of the fluid and the porous medium are constant, (iii) the Boussinesq approximation is employed, and (iv) Darcy's law is applicable, the governing equations in terms of stream function  $\hat{\psi}$  and temperature  $\hat{T}$  are [7]

$$\nabla^2 \hat{\psi} + (\rho_\infty g \beta K / \mu) \hat{T}_x = 0, \quad (1)$$

$$\hat{\psi}_y \hat{T}_x - \hat{\psi}_x \hat{T}_y = \alpha \nabla^2 \hat{T} \quad (2)$$

where  $\rho_\infty$ ,  $\mu$ , and  $\beta$  are the density, viscosity, and the thermal expansion coefficient of the fluid;  $K$  and  $\alpha$  are the permeability and the equivalent thermal diffusivity of the saturated porous medium;  $g$  is the gravitational acceleration and  $\hat{\psi}$ , the stream function, is defined as

$$\hat{u} = \hat{\psi}_y, \quad \hat{v} = -\hat{\psi}_x. \quad (3)$$

The boundary conditions for the problem are

$$\hat{y} = 0, \quad \hat{\psi} = 0, \quad \hat{T} = \hat{T}_\infty + A\hat{x}^\lambda, \quad (\hat{x} \geq 0), \quad (4a,b)$$

$$\hat{y} \rightarrow \infty, \quad \hat{\psi}_y = 0, \quad \hat{T} = \hat{T}_\infty. \quad (5a,b)$$

We now introduce the following dimensionless variables:

$$x = \hat{x}/L, \quad y = \hat{y}/L, \quad \psi = \hat{\psi}/(\alpha Ra), \quad (6)$$

$$\theta = (\hat{T} - \hat{T}_\infty)/\Delta \hat{T}, \quad (7)$$

where  $L$  is a characteristic length,  $\Delta \hat{T} = A L^\lambda$ , and  $Ra$  is the Rayleigh number defined as  $Ra = \rho_\infty g \beta K \Delta \hat{T}_r L / \mu \alpha$ . The dimensionless velocity components are given by

$$u = [L/(\alpha Ra)] \hat{u} = \psi_y, \quad v = [L/(\alpha Ra)] \hat{v} = -\psi_x. \quad (7)$$

In terms of the dimensionless variables, the governing equations (1)–(4) become

$$\nabla^2 \psi + \theta_x = 0, \quad (8)$$

$$\psi_y \theta_x - \psi_x \theta_y = (1/Ra) \nabla^2 \theta, \quad (9)$$

with boundary conditions

$$y = 0, \quad \psi = 0, \quad \theta = x^\lambda, \quad x \geq 0 \quad (10a,b)$$

$$y \rightarrow \infty, \quad \psi_y = 0, \quad \theta = 0. \quad (11a,b)$$

The asymptotic solutions to equations (8)–(11) will now be sought for large values of  $Ra$  ( $Ra \gg 1$ ),

The limit of  $Ra \rightarrow \infty$  corresponds to exposing the heated surface in a porous medium saturated with a non-heat conducting fluid. Thus, there will be no heat transfer and the temperature distribution will be given

by

$$y > 0, \quad \theta = 0, \quad \text{as } Ra \rightarrow \infty, \quad (12a)$$

$$y = 0, \quad \theta = \begin{cases} x^\lambda, & x \geq 0 \\ 0, & x < 0 \end{cases} \text{ as } Ra \rightarrow \infty. \quad (12b)$$

Furthermore, since no fluid motion is generated

$$\psi = 0, \quad \text{when } Ra \rightarrow \infty. \quad (13)$$

In view of equations (12a) and (13), we now write the straightforward (outer) expansions of  $\psi$  and  $\theta$  as

$$\psi(x, y, \varepsilon) = \varepsilon^2[\psi_1(x, y) + \varepsilon\psi_2(x, y) + \dots], \quad (14a)$$

$$\theta(x, y, \varepsilon) = \varepsilon[\theta_1(x, y) + \varepsilon\theta_2(x, y) + \dots], \quad (14b)$$

where  $\varepsilon \equiv (Ra)^{-1/3}$ . It follows from equation (14a) that the outer expansions for the velocity components are

$$u(x, y; \varepsilon) = \varepsilon^2[u_1(x, y) + \varepsilon u_2(x, y) + \dots], \quad (15a)$$

$$v(x, y; \varepsilon) = \varepsilon^2[v_1(x, y) + \varepsilon v_2(x, y) + \dots], \quad (15b)$$

where  $u_i = \partial\psi_i/\partial y$  and  $v_i = -\partial\psi_i/\partial x$  ( $i = 1, 2, \dots, N$ ).

*The inner solution*

A thermal layer is required to remove the temperature jump at the heated surface. We therefore introduce the following inner expansions:

$$\psi(x, y; \varepsilon) = \varepsilon^2[\Psi_0(X, Y) + \varepsilon\Psi_1(X, Y) + \varepsilon^2\Psi_2(X, Y) + \dots + \varepsilon^{2m}\Psi_m(X, Y)], \quad (16a)$$

$$\theta(x, y; \varepsilon) = \Theta_0(X, Y) + \varepsilon\Theta_1(X, Y) + \varepsilon^2\Theta_2(X, Y) + \dots + \varepsilon^{2m}\Theta_m(X, Y) \quad (16b)$$

with the inner variables given by

$$X = x \quad \text{and} \quad Y = y/\varepsilon \quad (17)$$

where  $\Psi_m$  and  $\Theta_m$  are the eigensolutions associated with the homogeneous equations and boundary conditions and the  $\alpha_m$ 's are the corresponding eigenvalues. It will be shown later in this paper that  $\alpha_m = 2$  and  $3$  for  $\lambda = 0$  while no eigenvalue exists for  $\lambda > 0.1$ . It follows from equation (16a) that the inner expansions of the velocity components are

$$u(x, y; \varepsilon) = \varepsilon[U_0(X, Y) + \varepsilon U_1(X, Y) + \varepsilon^2 U_2(X, Y) + \dots + \varepsilon^{2m} U_m], \quad (18a)$$

$$v(x, y; \varepsilon) = \varepsilon^2[V_0(X, Y) + \varepsilon V_1(X, Y) + \varepsilon^2 V_2(X, Y) + \dots + \varepsilon^{2m} V_m] \quad (18b)$$

where  $U_i = \Psi_{iY}$ , and  $V_i = -\Psi_{iX}$  ( $i = 1, 2, \dots, N$ ). (19)

Rewriting equations (8) and (9) in terms of inner variables given by equations (17), and upon substitution of equations (16), we find the following sets of inner problems:

*The first-order inner problem.*

$$\Psi_{0YY} + \Theta_{0X} = 0, \quad (20a)$$

$$\Psi_{0Y}\Theta_{0X} - \Psi_{0X}\Theta_{0Y} = \Theta_{0YY}, \quad (20b)$$

subject to the boundary conditions

$$Y = 0, \quad \Psi_0 = 0, \quad \Theta_0 = X^\lambda, \quad (21a,b)$$

$$Y \rightarrow \infty, \quad \Psi_{0Y} = 0, \quad \Theta_0 = 0. \quad (22a,b)$$

Note that the first-order problem, given by equations (20)–(22), is exactly the same set of equations obtained from the boundary layer approximations [1]. A detailed examination of equation (20a) implies that  $\partial u/\partial y \gg \partial v/\partial x$  (and consequently the vorticity  $\nabla^2\psi \equiv \partial u/\partial y - \partial v/\partial x \simeq \partial u/\partial y$ ) which means that in the Darcy's law the upward-drift induced friction term,  $\mu \dot{v}/K$ , is neglected in comparison with the streamwise friction term  $\mu \dot{u}/K$  to this order. Moreover, equation (20b) implies that the streamwise heat conduction has been neglected.

*The second-order inner problem.*

$$\Psi_{1YY} + \Theta_{1X} = 0, \quad (23a)$$

$$(\Psi_{0Y}\Theta_{1X} - \Psi_{0X}\Theta_{1Y}) + (\Psi_{1Y}\Theta_{0X} - \Psi_{1X}\Theta_{0Y}) = \Theta_{1YY}, \quad (23b)$$

subject to the boundary conditions

$$Y = 0, \quad \Psi_1 = 0, \quad \Theta_1 = 0, \quad (24a,b)$$

$$Y \rightarrow \infty, \Psi_{1Y} \text{ and } \Theta_1 \text{ match with the outer solution.} \quad (25a,b)$$

Thus, to the second-order approximation, the vorticity is still equal to  $\partial u/\partial y$  while the streamwise heat conduction is still neglected in the energy equation. The nonlinear convection terms in equation (23b) are corrected for both the modified flow and temperature fields while the boundary conditions, equations (25a) and (25b), indicate the interaction between the inner and outer flow fields.

*The third-order inner problem.*

$$\Psi_{2YY} + \Theta_{2X} = -\Psi_{0XX}, \quad (26a)$$

$$(\Psi_{0Y}\Theta_{2X} - \Psi_{0X}\Theta_{2Y}) + (\Psi_{1Y}\Theta_{1X} - \Psi_{1X}\Theta_{1Y}) + (\Psi_{2Y}\Theta_{0X} - \Psi_{2X}\Theta_{0Y}) = \Theta_{0XX} + \Theta_{2YY}, \quad (26b)$$

subject to the boundary conditions

$$Y = 0, \quad \Psi_2 = 0, \quad \Theta_2 = 0, \quad (27a,b)$$

$$Y \rightarrow \infty, \Psi_{2Y} \text{ and } \Theta_2 \text{ match with the outer solution.} \quad (28a,b)$$

From the above equations, we observe that the vorticity term in equation (26a) has been corrected to include the contribution of  $\partial v/\partial x$  while the streamwise heat conduction term has been taken into account in equation (26b). Moreover, both the convection terms in the energy equation and the interaction between the outer and inner flow fields are further modified.

The eigenfunctions  $\Psi_m$  and  $\Theta_m$  satisfy the homogeneous problem given by

$$\Psi_{mYY} + \Theta_{mX} = 0, \quad (29a)$$

$$(\Psi_{0Y}\Theta_{mX} - \Psi_{0X}\Theta_{mY}) + (\Theta_{0X}\Psi_{mY} - \Theta_{0Y}\Psi_{mX}) = \Theta_{mYY}, \quad (29b)$$

subject to the boundary conditions

$$Y = 0: \quad \Psi_m = 0, \quad \Theta_m = 0, \quad (30a,b)$$

$$Y \rightarrow \infty: \quad \Psi_{mY} = 0, \quad \Theta_m = 0. \quad (31a,b)$$

The first-order inner solution. The solution of the first-order inner problem has been shown by Cheng and Chang [1] to be of the form

$$\Psi_0 = X^{(\lambda+1)/3} f_0(\eta), \quad (32a)$$

$$\Theta_0 = X^\lambda g_0(\eta), \quad (32b)$$

$$\eta = YX^{(\lambda-2)/3} \quad (32c)$$

where  $f_0(\eta)$  and  $g_0(\eta)$  are determined from

$$f_0'' + \lambda g_0 + [(\lambda-2)/3]\eta g_0' = 0, \quad (33a)$$

$$g_0'' - \lambda f_0' g_0 + [(\lambda+1)/3]f_0 g_0' = 0, \quad (33b)$$

with boundary conditions given by

$$g_0(0) = 1, \quad f_0(0) = 0, \quad (34a,b)$$

$$g_0(\infty) = 0, \quad f_0'(\infty) = 0. \quad (35a,b)$$

It follows from equation (32a) that the velocities are given by

$$U_0 = \frac{\partial \Psi_0}{\partial Y} = X^{(2\lambda-1)/3} f_0'(\eta), \quad (36a)$$

$$V_0 = -\frac{\partial \Psi_0}{\partial X} = -(X^{(\lambda-2)/3}/3)[(2-\lambda)\eta f_0' - (\lambda+1)f_0]. \quad (36b)$$

The asymptotic behavior of  $g_0(\eta)$  and  $f_0(\eta)$  are found from equation (33) to be of the form

$$g_0(\eta) \sim e^{-\gamma\eta} \quad (37a)$$

$$f_0(\eta) \sim f_0(\infty) + c_1 e^{-\gamma\eta} + c_2 \eta e^{-\gamma\eta} \quad (37b)$$

where  $\gamma \equiv [(\lambda+1)/3]f_0(\infty)$  with  $f_0(\infty)$  being a positive constant [1]. Hence, as  $\eta \rightarrow \infty$ , we have

$$\Psi_0 \sim X^{(\lambda+1)/3} f_0(\infty) + O(e^{-\gamma\eta}), \quad (38a)$$

$$\Theta_0 \sim O(e^{-\gamma\eta}), \quad (38b)$$

$$U_0 \sim O(e^{-\gamma\eta}), \quad (38c)$$

$$V_0 \sim -[(\lambda+1)/3]f_0(\infty)X^{(\lambda-2)/3}, \quad X \geq 0. \quad (38d)$$

Equation (38d) shows that at the edge of the thermal layer, the vertical velocity is negative. This implies that fluid is entrained into the thermal layer, i.e. streamlines are all entering from the outside into the boundary layer. Note that to the first-order theory,  $\lambda = 0.5$  corresponds to the case of constant surface heat flux [1].

The outer solution

By substituting equation (14) into equations (8) and (9), the following sets of equations are obtained:

First-order outer problem.

$$\theta_{1x} = 0, \quad (39)$$

$$\psi_{1y}\theta_{1x} - \psi_{1x}\theta_{1y} = 0. \quad (40)$$

Second-order outer problem.

$$\nabla^2 \psi_1 + \theta_{2x} = 0, \quad (41)$$

$$(\psi_{1y}\theta_{2x} - \psi_{1x}\theta_{2y}) + (\psi_{2y}\theta_{1x} - \psi_{2x}\theta_{1y}) = \nabla^2 \theta_1. \quad (42)$$

Nth-order outer problem.

$$\nabla^2 \Psi_{n-1} + \theta_{nx} = 0, \quad (n = 2, 3, \dots, N) \quad (43)$$

$$\begin{aligned} &\psi_{1y}\theta_{nx} - \psi_{1x}\theta_{ny} \\ &= \nabla^2 \theta_{n-1} - \sum_{j=1}^{n-1} [\psi_{n-j+1,y}\theta_{jx} - \psi_{n-j+1,x}\theta_{jy}], \end{aligned} \quad (n = 2, 3, \dots, N). \quad (44)$$

The boundary conditions for all orders ( $n = 1, 2, \dots, N$ ) are:

$$y = 0, \theta_n \text{ and } \psi_n \text{ match with the inner solutions at the edge of the thermal layer,} \quad (45a)$$

$$y \rightarrow \infty, \theta_n = 0, \psi_{ny} = \psi_{nx} = 0. \quad (45b)$$

Equation (39) shows that  $\theta_1$  is a function of  $y$  only and therefore must be equal to zero by equation (45b). Another more general argument for  $\theta_1 = 0$  is based on equation (40), which shows that  $\theta_1$  is constant along any of the first-order outer streamlines  $\psi_1$ . As pointed out earlier the first-order streamlines are entering the boundary layer and none leaving it,  $\psi_1$  may be originated from infinity or form closed loops in the region outside the thermal layer. Excluding the latter possibility, all are originated from infinity where  $\theta_1 = 0$ . Hence by equation (40) and the infinity condition  $\theta_1 = 0$ , we conclude that  $\theta_1 = 0$  everywhere. With  $\theta_1 = 0$ , the second order equation (42) reduces to

$$\psi_{1y}\theta_{2x} - \psi_{1x}\theta_{2y} = 0,$$

from which, by the same argument, we conclude that  $\theta_2 = 0$  everywhere. Hence, by induction, we find that in the outer region

$$\theta_n = 0, \text{ everywhere for all } n \quad (46a)$$

and

$$\nabla^2 \psi_n = 0 \text{ for all } n. \quad (46b)$$

In other words, in the outer flow field both temperature perturbation and vorticity are exponentially small and a potential flow prevails. The first-order outer solution is therefore determined by the equation

$$\nabla^2 \psi_1 = 0, \quad (47)$$

subject to the infinity condition  $\psi_{1x} = \psi_{1y} = 0$  and the matching condition given by equation (38a), i.e.

$$\psi_1(x, 0) = \begin{cases} f_0(\infty)x^{(\lambda+1)/3} & x \geq 0, \\ 0 & x < 0. \end{cases} \quad (48)$$

The solution of equation (47) with boundary conditions (48) can be shown to be

$$\psi_1 = -\{c/[(m-1)r^{m-1}]\}\sin[m(\pi-\Lambda)+\Lambda] \quad (49)$$

where  $r = (x^2 + y^2)^{1/2}$ ,  $\Lambda = \tan^{-1}(y/x)$ ,  $c = [(1+\lambda)/3][f_0(\infty)/(\sin m\pi)]$  and  $m = (2-\lambda)/3$ . It follows from

equation (49) that

$$u_1 = [c \cos m(\pi - \Lambda)]/(r^m), \quad (50a)$$

$$v_1 = -[c \sin m(\pi - \Lambda)]/(r^m). \quad (50b)$$

The second-order inner solution. The governing equations and boundary conditions for the second-order inner problem are given by equations (23) and (24) with the matching condition

$$\frac{\partial \Psi_1}{\partial Y}(X, \infty) = DX^{(\lambda-2)/3}, \quad (51a)$$

$$\Theta_1(X, \infty) = 0 \quad (51b)$$

where  $D = -[(1 + \lambda)/3] \cot\{[(\lambda + 1)/3]\pi\} f_0(\infty)$ . Note that equations (51) are obtained from equations (50a) and (46a). It can be shown that the second-order inner problem admits similarity solutions of the form

$$\Psi_1 = Df_1(\eta), \quad (52a)$$

$$\Theta_1 = DX^{(2\lambda-1)/3} g_1(\eta) \quad (52b)$$

where  $f_1(\eta)$  and  $g_1(\eta)$  are determined from

$$f_1'' + [(2\lambda - 1)/3]g_1 + [(\lambda - 2)/3]\eta g_1' = 0, \quad (53a)$$

$$g_1'' + [(\lambda + 1)/3]f_0 g_1' - [(2\lambda - 1)/3]f_0' g_1 = \lambda g_0 f_1', \quad (53b)$$

subject to the boundary conditions

$$f_1(0) = g_1(0) = 0, \quad (54a,b)$$

$$f_1'(\infty) = 1, \quad g_1(\infty) = 0. \quad (55a,b)$$

From equations (51) and (52) it is of interest to note that  $\Psi_1(X, Y) = \Theta_1(X, Y) = 0$  for the special case of  $\lambda = 0.5$ , since  $D = 0$  for this case. The asymptotic behavior of  $g_1(\eta)$  and  $f_1(\eta)$  can be found from equations (53) and (55) which gives

$$\eta \rightarrow \infty, \quad g_1(\eta) \sim e^{-\eta} \quad \text{and} \quad f_1(\eta) \sim \eta + C \quad (56a,b)$$

where  $C$  is a constant (whose value depends on  $\lambda$ ) and can be obtained only after equations (53)–(55) have been solved numerically.

Thus, to this order, the inner expansion for the stream function is

$$\begin{aligned} \psi(x, y) &= \varepsilon^2 [\Psi_0(x, Y) + \varepsilon \Psi_1(x, Y) + \dots] \\ &= \varepsilon^2 [X^{(\lambda+1)/3} f_0(\eta) + \varepsilon D f_1(\eta) + \dots]. \end{aligned} \quad (57)$$

It follows that as  $\eta \rightarrow \infty$ ,

$$\begin{aligned} \psi(x, y) &= \varepsilon^2 \{ X^{(\lambda+1)/3} f_0(\infty) \\ &\quad + \varepsilon D [X^{(\lambda-2)/3} Y + C] + \dots \} \end{aligned} \quad (58)$$

where we have made use of equation (56b). Equation (58) is to be matched with the outer expansion in the next section.

Second-order outer solution. The governing equation for the second-order outer problem is

$$\nabla^2 \psi_2 = 0 \quad (59)$$

with the boundary conditions

$$\psi_2(x, 0) = \begin{cases} DC, & x \geq 0 \\ 0, & x < 0 \end{cases} \quad (60a)$$

$$(60b)$$

and the infinity conditions

$$\psi_{2x}(x, \infty) = \psi_{2y}(x, \infty) = 0 \quad (61a,b)$$

where equation (60a) is obtained by matching with the inner solution. It is easy to show that the solution to equation (59) with the boundary conditions (60) and (61) is

$$\psi_2(x, y) = DC [1 - (\Lambda/\pi)] = DC [1 - (1/\pi) \tan^{-1}(y/x)]. \quad (62)$$

Expanding equation (62) for small  $y$ , we have

$$\begin{aligned} \psi_2(x, y) &= DC [1 - (1/\pi)(y/x) + \dots] \\ &= DC [1 - (\varepsilon Y/\pi X) + \dots]. \end{aligned} \quad (63)$$

Thus the velocity  $u$  (as  $y \rightarrow 0$ ) to the second order is

$$\begin{aligned} u &= \varepsilon^2 [u_1(x, y) + \varepsilon u_2(x, y) + \dots] \\ &= -\varepsilon^2 [(\lambda + 1)/3] \cot\{[(\lambda + 1)/3]\pi\} f_0(\infty) x^{(\lambda-2)/3} \\ &\quad + \varepsilon^3 \{ [(\lambda + 1)(2 - \lambda)/9] f_0(\infty) x^{(\lambda-5)/3} Y \\ &\quad - (DC/\pi)(1/x) \} + O(\varepsilon^4). \end{aligned} \quad (64)$$

The third-order inner solution. The third-order inner solution, as determined from equations (26) and (27) must also satisfy the matching condition at  $Y \rightarrow \infty$

$$\Theta_2 \rightarrow 0, \quad (65a)$$

$$\begin{aligned} U_2 = \frac{\partial \Psi_2}{\partial Y} &= [(1 + \lambda)(2 - \lambda) f_0(\infty) Y X^{(\lambda-5)/3} / 9] \\ &\quad - (DC/\pi)(1/X) \end{aligned} \quad (65b)$$

where equation (65b) is obtained by matching with equation (64). Equations (26) with the boundary conditions (27) and (65) admit similarity solutions of the form

$$\Psi_2 = X^{-(\lambda+1)/3} f_2(\eta), \quad (66a)$$

$$\Theta_2 = X^{(\lambda-2)/3} g_2(\eta) \quad (66b)$$

where  $\eta$  is the similarity variable given by equation (32c), and  $f_2(\eta)$  and  $g_2(\eta)$  are determined from

$$\begin{aligned} f_2'' + [(\lambda - 2)/3](g_2 + \eta g_2') \\ = -[(\lambda - 2)/3] \{ [(\lambda + 1)/3] f_0 + (\lambda - 1) \eta f_0' \\ + [(\lambda - 2)/3] \eta^2 f_0'' \}, \end{aligned} \quad (67a)$$

$$\begin{aligned} g_2'' + \frac{1}{3} [(\lambda + 1) f_0 g_2' - (\lambda - 2) f_0' g_2] \\ - \lambda f_2' g_0 - [(1 + \lambda)/3] f_2 g_0' = \lambda(1 - \lambda) g_0 \\ + [(1 - 2\lambda)(\lambda - 2)/3] \eta g_0' - [(\lambda - 2)/3]^2 \eta (g_0' + \eta g_0'') \\ + [(2\lambda - 1)/3] [(1 + \lambda)/3]^2 \\ \times \cot^2 \{ [(\lambda + 1)/3] \pi \} f_0^2(\infty) f_1' g_1, \end{aligned} \quad (67b)$$

subject to the boundary conditions

$$\eta = 0: \quad f_2 = 0, \quad g_2 = 0, \quad (68a,b)$$

$$\eta \rightarrow \infty : f_2' = [(1 + \lambda)(2 - \lambda)/9]f_0(\infty)\eta - (DC/\pi); \quad 3\lambda/(\lambda + 1) = \alpha_m + [3\Gamma/(\lambda + 1)]. \quad (82)$$

$$g_2 = 0. \quad (69a,b) \quad \text{Solving equations (81) and (82), we have}$$

*Eigenvalues and eigenfunctions*

In this section, we shall obtain the eigenvalues  $\alpha_m$  and the eigenfunctions  $\Psi_m$  and  $\Theta_m$ . To this end, we note that the parameter  $Ra$  in equations (8)–(11) is an artificial parameter that can be eliminated from the mathematical problem by the following transformation:

$$\psi = \varepsilon^3 \bar{\psi}, \quad \theta = \varepsilon^{3\lambda/(\lambda+1)} \bar{\theta} \quad (70a,b)$$

$$x = \varepsilon^{3/(\lambda+1)} \bar{x}, \quad y = \varepsilon^{3/(\lambda+1)} \bar{y} \quad (70c,d)$$

where  $\varepsilon = (1/Ra)^{1/3}$ . In terms of the new variables, equations (8)–(11) become

$$\nabla^2 \bar{\psi} + \bar{\theta}_{\bar{x}} = 0 \quad (71)$$

$$\bar{\psi}_{\bar{y}} \bar{\theta}_{\bar{x}} - \bar{\psi}_{\bar{x}} \bar{\theta}_{\bar{y}} = \bar{\nabla}^2 \bar{\theta} \quad (72)$$

with boundary conditions given by

$$\bar{y} = 0 : \quad \bar{\psi} = 0, \quad \bar{\theta} = \bar{x}^{\lambda} \quad \bar{x} \geq 0, \quad (73a,b)$$

$$\bar{y} \rightarrow \infty : \quad \bar{\psi}_{\bar{y}} = 0, \quad \bar{\theta} = 0. \quad (74a,b)$$

An inspection of equations (71)–(74) shows that the parameter  $\varepsilon$  (or  $Ra$ ) is completely eliminated from the problem. In other words, we have

$$\bar{\psi} = \bar{\psi}(\bar{x}, \bar{y}), \quad (75)$$

$$\bar{\theta} = \bar{\theta}(\bar{x}, \bar{y}), \quad (76)$$

which imply that the parameter  $\varepsilon$  should not appear in the solution when it is expressed in terms of the new variables. This is the so-called “eliminability principle”.

We now consider the terms  $\varepsilon^{2m+2}\psi_m$  and  $\varepsilon^{2m}\theta_m$  in equations (16). These terms can be considered at present to be the typical terms in the series expansions. We assume that these terms are of the following similarity forms:

$$\varepsilon^{2m+2}\Psi_m = \varepsilon^{2m+2}x^\sigma f_m(\eta), \quad (77)$$

$$\varepsilon^{2m}\Theta_m = \varepsilon^{2m}x^\Gamma g_m(\eta) \quad (78)$$

where  $\eta = x^{(\lambda-2)/3}y/\varepsilon$  and  $\sigma$  and  $\Gamma$  are constants to be determined. According to the eliminability principle, equation (16) in terms of  $\bar{\psi}$ ,  $\bar{\theta}$ ,  $\bar{x}$  and  $\bar{y}$  should not contain the parameter  $\varepsilon$ . We first note that the similarity variable  $\eta$  in terms of  $\bar{x}$  and  $\bar{y}$  becomes

$$\eta = \bar{x}^{(\lambda-2)/3} \bar{y} \quad (79)$$

where  $\varepsilon$  indeed disappears. Next, we rewrite the series (16a,b) in terms of  $\bar{\psi}$ ,  $\bar{\theta}$ ,  $\bar{x}$  and  $\bar{y}$  to give

$$\varepsilon^3 \bar{\psi} = \dots \varepsilon^{2m+2} \Psi_m = \dots$$

$$\varepsilon^{2m+2 + [3\sigma/(\lambda+1)]} \bar{x}^\sigma f_m(\eta), \quad (80a)$$

$$\varepsilon^{3\lambda/(\lambda+1)} \bar{\theta} = \dots \varepsilon^{2m} \Theta_m = \dots$$

$$\varepsilon^{2m + [3\Gamma/(\lambda+1)]} \bar{x}^\Gamma g_m(\eta). \quad (80b)$$

The parameter  $\varepsilon$  will not appear in the above equations if

$$3 = \alpha_m + 2 + [3\sigma/(\lambda + 1)], \quad (81)$$

$$\sigma = (1 - \alpha_m)(\lambda + 1)/3, \quad (83)$$

$$\Gamma = \lambda - [(1 + \lambda)\alpha_m/3]. \quad (84)$$

Thus, typical terms in the series of equation (16a) and (16b) are given by

$$\Psi_m = x^{(1 - \alpha_m)(\lambda + 1)/3} f_m(\eta), \quad (85)$$

$$\Theta_m = x^{\lambda - [(1 + \lambda)\alpha_m/3]} g_m(\eta). \quad (86)$$

Letting  $\alpha_m = 0, 1$ , and  $2$ , in equations (85) and (86), a linear combination of these terms gives,

$$\psi = \varepsilon^2 [A_0 x^{(\lambda+1)/3} f_0(\eta) + \varepsilon A_1 f_1(\eta) + \varepsilon^2 A_2 x^{-(\lambda+1)/3} f_2(\eta) + \dots + A_m \varepsilon^{2m} x^{(1 - \alpha_m)(\lambda + 1)/3} f_m(\eta) + \dots], \quad (87a)$$

$$\theta = [B_0 x^\lambda g_0(\eta) + \varepsilon B_1 x^{(2\lambda-1)/3} g_1(\eta) + \varepsilon^2 B_2 x^{(\lambda-2)/3} g_2(\eta) + \dots + B_m \varepsilon^{2m} x^{\lambda - [(1 + \lambda)\alpha_m/3]} g_m(\eta) + \dots] \quad (87b)$$

where  $A_0, A_1, B_0$  and  $B_1$ , are constants to be determined. Note that the first three terms in equations (87) agree with equations (29), (49), and (63) if  $A_0 = A_2 = B_0 = B_2 = 1$  and  $A_1 = B_1 = D$ . The constants  $A_m$  and  $B_m$  in equations (87) cannot be determined presumably due to the leading edge effects.

Substituting equations (77) and (78) with  $\sigma$  and  $\Gamma$  given by equations (83) and (84) into equations (29)–(31), we have the following eigenvalue problem:

$$f_m'' + \{\lambda - [(\lambda + 1)x_m/3]\}g_m + [(\lambda - 2)/3]\eta g_m' = 0, \quad (88)$$

$$g_m'' + [(\lambda + 1)/3]f_0 g_m' - \{\lambda - [(\lambda + 1)x_m/3]\}f_0' g_m - \lambda g_0 f_m' - [(\alpha_m - 1)(\lambda + 1)/3]g_0' f_m = 0 \quad (89)$$

subject to the boundary conditions

$$f_m(0) = g_m(0) = 0, \quad (90a,b)$$

$$f_m'(\infty) = g_m(\infty) = 0. \quad (91a,b)$$

As in the classical boundary layer theory it will now be shown that  $\partial\Psi_0/\partial X$  and  $\partial\Theta_0/\partial X$  or  $\partial\Psi_0/\partial Y$  and  $\partial\Theta_0/\partial Y$  satisfy equations (29) and thus are the eigenfunctions, provided that they also satisfy the boundary conditions (30) and (31). For this reason, we first differentiate equations (20) with respect to  $X$  and find that the resulting equations are identical to equations (29) if

$$\Psi_m = \frac{\partial\Psi_0}{\partial X} = X^{(\lambda-2)/3} \{[(\lambda + 1)/3]f_0(\eta) + [(\lambda - 2)/3]f_0'(\eta)\}, \quad (92a)$$

$$\Theta_m = \frac{\partial\Theta_0}{\partial X} = X^{\lambda-1} \{\lambda g_0(\eta) + [(\lambda - 2)/3]\eta g_0'\}. \quad (92b)$$

Comparing equations (92) with equations (85) and (86), one obtains

$$\alpha_m = 3/(\lambda + 1), \quad (93a)$$

$$f_m = [(\lambda + 1)/3]f_0(\eta) + [(\lambda - 2)/3]f'_0(\eta), \quad (93b)$$

$$g_m = \lambda g_0(\eta) + [(\lambda - 2)/3]\eta g'_0(\eta). \quad (93c)$$

Equations (93a,b) satisfy boundary conditions (90) and (91) only when  $\lambda = 0$ . Thus, when  $\lambda = 0$ , the eigenfunctions and eigenvalues are

$$\Psi_m = X^{-2/3}[(f_0(\eta)/3) - \frac{2}{3}\eta f'_0(\eta)], \quad (94a)$$

$$\Theta_m = X^{-1}[-\frac{2}{3}\eta g'_0], \quad (94b)$$

$$\alpha_m = 3. \quad (95)$$

Similarly, it can be shown that although  $\partial\Psi_0/\partial Y$  and  $\partial\Theta_0/\partial Y$  satisfy equations (29), they do not satisfy boundary conditions (30) and (31) and thus are not eigenfunctions of the problem. Other eigenvalues and eigenfunctions must be found by the numerical integration of equations (88)–(91).

*Results and discussion*

Numerical solutions for the eigenvalue problem given by equations (88)–(91) were carried out for  $\lambda = 0, 0.1, 0.5, 1.0$  and  $1.5$ . It was found that for  $\lambda = 0$ , two eigenvalues with  $\alpha_m = 2$  and  $3$  exist. This implies that the third-order problem for this case contains an indetermined constant due to the leading edge effects. The numerical solutions also found that no other eigenvalues exist for  $\lambda \geq 0.1$ . Thus, for  $\lambda = 0$ , numerical solutions were carried out only to the second-order while for other values of  $\lambda$ , numerical solutions were carried out to the third-order. The results for  $g'_i(0)$  and  $f'_i(0)$  (with  $i = 0, 1, 2$ ) and  $f_0(\infty)$  for selected values of  $\lambda$  are tabulated in Table 1 for future reference. The discussion of the first-order (boundary layer) results has been presented in the previous work [1] and will not be repeated here.

*The second-order theory.* The variations of  $g_1, g'_1, f_1$  and  $f'_1$  versus  $\eta$  at different  $\lambda$  are presented in Figs. 1–4. Note that for the special case of  $\lambda = 0$ , the second-order equation and boundary conditions for  $g_1$  as given by equations (53b), (54b) and (55b) become a linear homogeneous problem whose exact solution is

$$g_1 = 0 \quad \text{and} \quad g'_1 = 0. \quad (96a,b)$$

It follows from equation (53a), (54a), and (55a) that

$$f'_1 = 1 \quad \text{and} \quad f_1 = \eta. \quad (97a,b)$$

Comparing equation (97b) with equation (56b), one can conclude that  $C = 0$  for  $\lambda = 0$ . Equations (96) and (97a) are shown as horizontal lines in Figs. 1, 2 and 4

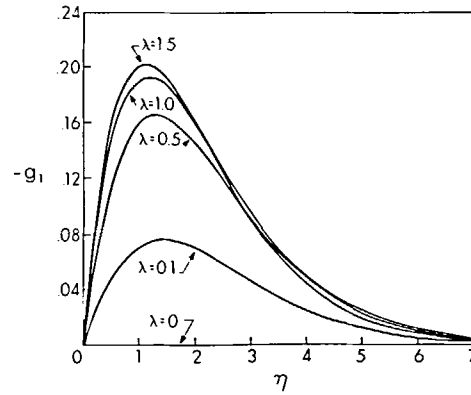


FIG. 1.  $g_1$  versus  $\eta$  at selected values of  $\lambda$ .

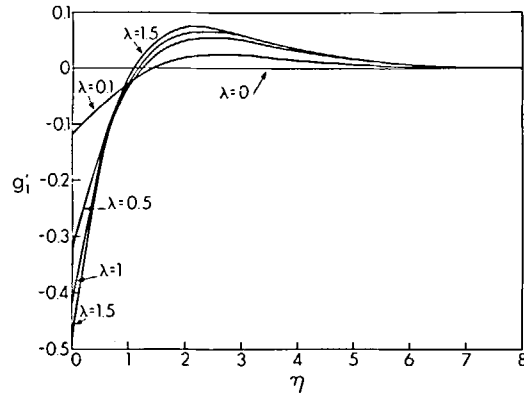


FIG. 2.  $g'_1$  versus  $\eta$  at selected values of  $\lambda$ .

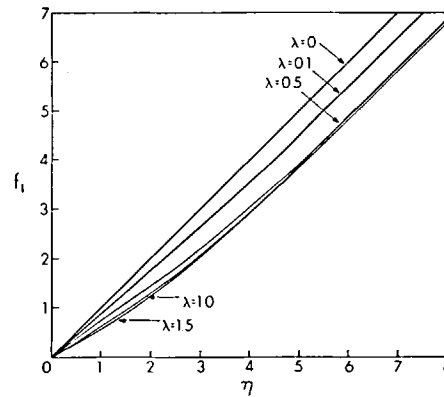


FIG. 3.  $f_1$  versus  $\eta$  at selected values of  $\lambda$ .

Table 1. Values of  $g'_i(0), f'_i(0)$  and  $f_0(\infty)$

	$\lambda = 0$	$\lambda = 0.1$	$\lambda = 0.5$	$\lambda = 1.0$	$\lambda = 1.5$
$g'_0(0)$	-0.4299	-0.5262	-0.8164	-1.099	-1.345
$g'_1(0)$	0	-0.1165	-0.3154	-0.4207	-0.4735
$g'_2(0)$		-0.2281	0	0.2274	0.9424
$f'_0(0)$	1.053	1.064	1.141	1.251	1.354
$f'_1(0)$	1.0	0.9108	0.7413	0.6182	0.5257
$f'_2(0)$		-0.07617	0	0.2292	0.6908
$f_0(\infty)$	2.813	2.529	1.885	1.502	1.284

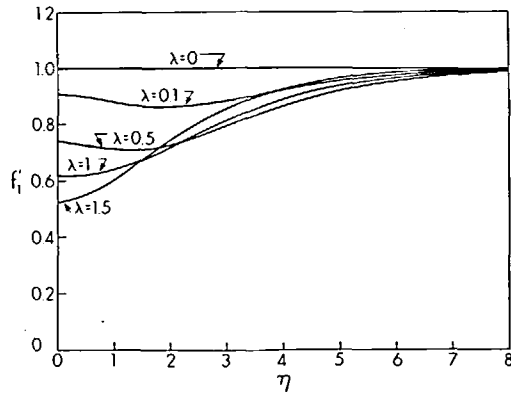


FIG. 4.  $f'_1$  versus  $\eta$  at selected values of  $\lambda$ .

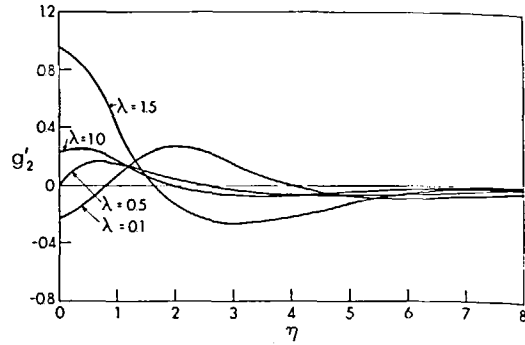


FIG. 6.  $g'_2$  versus  $\eta$  at selected values of  $\lambda$ .

while equation (97b) is shown as a straight line in Fig. 3. Note that equations (96) imply that the second-order corrections in temperature and heat flux are zero for  $\lambda = 0$  because to the second order approximation, the correction to the temperature,  $\Theta_1$ , is solely due to the convection effect as represented by the forcing term

$$\Psi_{1Y}\Theta_{0X} - \Psi_{1X}\Theta_{0Y}$$

in equation (23b). When  $\lambda = 0$ ,  $\Theta_0$  and  $\Psi_1$  are both constant along the curves  $\eta = \text{constant}$  [see equations (32b) and (52a)], and hence the above convection term vanishes. This, coupled with the boundary conditions  $\Theta_1 = 0$  at  $Y = 0$  [equation (24)] and  $\Theta_1 \rightarrow 0$ , as  $Y \rightarrow \infty$  [equation (51b)] leads to the result that  $\Theta_1 = 0$  for  $\lambda = 0$ .

As discussed earlier, the second-order corrections for the stream function and temperature,  $\Psi_1$  and  $\Theta_1$ , are also zero for  $\lambda = 0.5$  since  $D = 0$ . For completeness, however, the values of  $g_1, g'_1, f_1$ , and  $f'_1$  as determined from equations (53)–(55) for  $\lambda = 0.5$  are also plotted in Figs. 1–4, although they are of no physical significance. For other non-zero value of  $\lambda$ , Figs. 1 and 2 show that the second-order corrections in temperature and its slope at the wall are all negative while Figs. 3 and 4 show that the values of  $f_1$  and  $f'_1$  are all positive with  $f_1$  varying linearly with  $\eta$  as  $\eta \rightarrow \infty$  as indicated by equation (56b).

*The third-order theory.* Figures 5–8 show the third-order corrections,  $g_2, g'_2, f_2$  and  $f'_2$  versus  $\eta$  for  $\lambda = 0.1$ ,

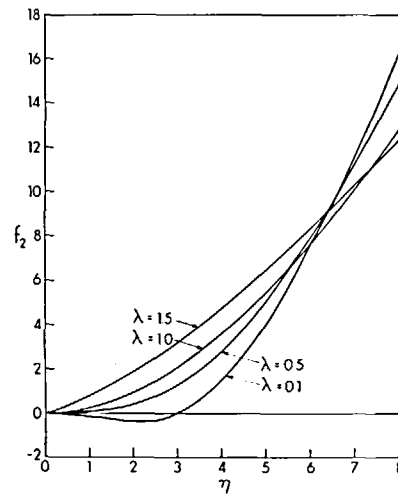


FIG. 7.  $f_2$  versus  $\eta$  at selected values of  $\lambda$ .

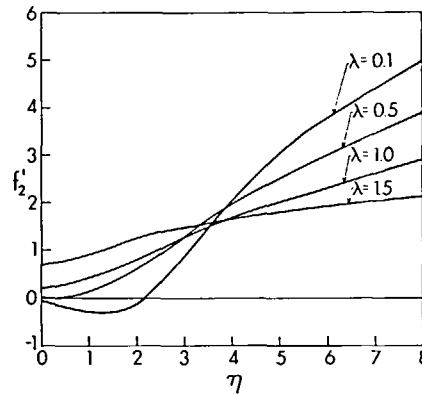


FIG. 8.  $f'_2$  versus  $\eta$  at selected values of  $\lambda$ .

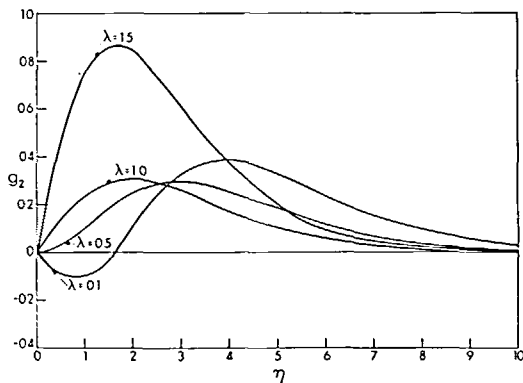


FIG. 5.  $g_2$  versus  $\eta$  at selected values of  $\lambda$ .

0.5, 1.0 and 1.5. As shown in Fig. 5, the values of  $g_2$  may be positive or negative depending on the values of  $\lambda$  and  $\eta$ . Figure 6 shows that  $g'_2(0) < 0$  for  $\lambda < 0.5$ , and  $g'_2(0) > 0$  for  $\lambda > 0.5$ . For  $\lambda \geq 0.5$ , the values of  $f_2$  and  $f'_2$  are all positive as shown in Figs. 7 and 8. Note that  $f'_2$  increases linearly with  $\eta$  as  $\eta \rightarrow \infty$  (see Fig. 8), which is dictated by the boundary condition (69a).



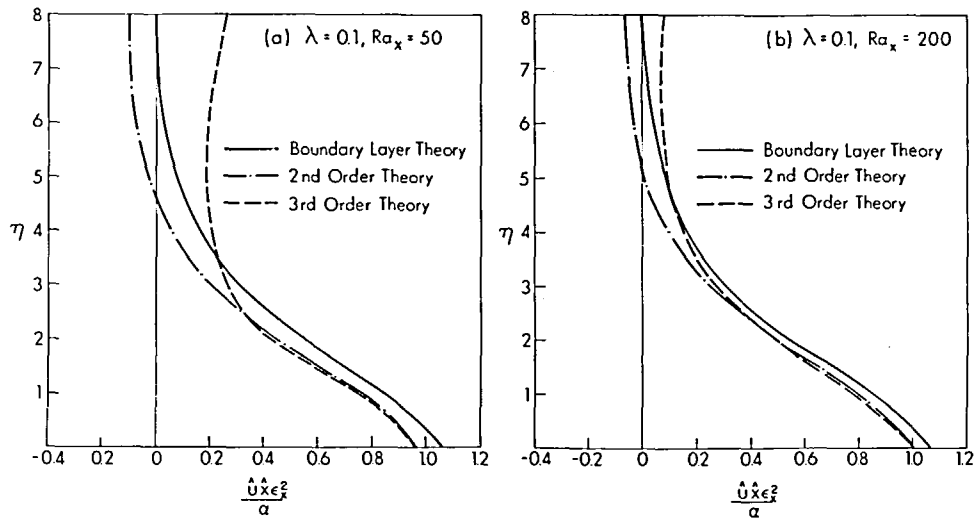


FIG. 9. Dimensionless horizontal velocity profiles for  $\lambda = 0.1$ : (a)  $Ra_x = 50$  and (b)  $Ra_x = 200$ .

*Higher-order corrections for the velocity field.* With the aid of equations (16a), (29a), (52a) and (66a), the inner expansion for the stream function is given by

$$\hat{\psi}(x, y) = (\alpha/\epsilon_x) \{ f_0(\eta) - \epsilon_x [(\lambda + 1)/3] \cot[\pi(\lambda + 1)/3] \times f_0(\infty) f_1(\eta) + \epsilon_x^2 f_2(\eta) + O(\epsilon_x^3) \} \quad (98)$$

where  $\epsilon_x \equiv Ra_x^{-1/3}$  with  $Ra_x \equiv \rho_\infty g \beta K (\hat{T}_w - \hat{T}_\infty) \hat{x} / \mu x$  denoting the local Rayleigh number. It follows that the horizontal velocity is

$$\epsilon_x^2 \hat{u} \hat{x} / \alpha = \{ f'_0(\eta) - \epsilon_x [(\lambda + 1)/3] \cot[\pi(\lambda + 1)/3] (\infty) f'_1(\eta) + \epsilon_x^2 f'_2(\eta) + O(\epsilon_x^3) \}. \quad (99)$$

Equations (98) and (99) are for  $\lambda > 0.1$ . For  $\lambda < 0.1$ , the third-order terms in these equations contain an undetermined constant as discussed earlier. Since  $f'_1(\eta) > 0$  and  $f_0(\infty) > 0$ , the second-order correction

in  $u$  is zero for  $\lambda = 0.5$ , negative for  $\lambda < 0.5$  and positive for  $\lambda > 0.5$ . On the other hand, the third-order corrections in  $u$  are almost always positive except for small  $\eta$  and  $\lambda < 0.5$ .

Figures 9(a) and 9(b) show the representative horizontal velocity profiles for  $\lambda < 0.5$  at two different Rayleigh numbers, as obtained from the first, second, and third-order theories. For the second-order theory, the horizontal velocity decreases from a positive value at the wall (i.e. a velocity slip) and approaches a negative value at the edge of the boundary layer. A comparison of Figs. 9(a) and 9(b) indicates that the boundary layer approximations become increasingly accurate as the value of  $Ra_x$  is increased. The representative horizontal velocity profiles for  $\lambda < 0.5$  are presented in Fig. 10. The major difference between this figure and Fig. 9 is that the horizontal velocity at the edge of the boundary layer

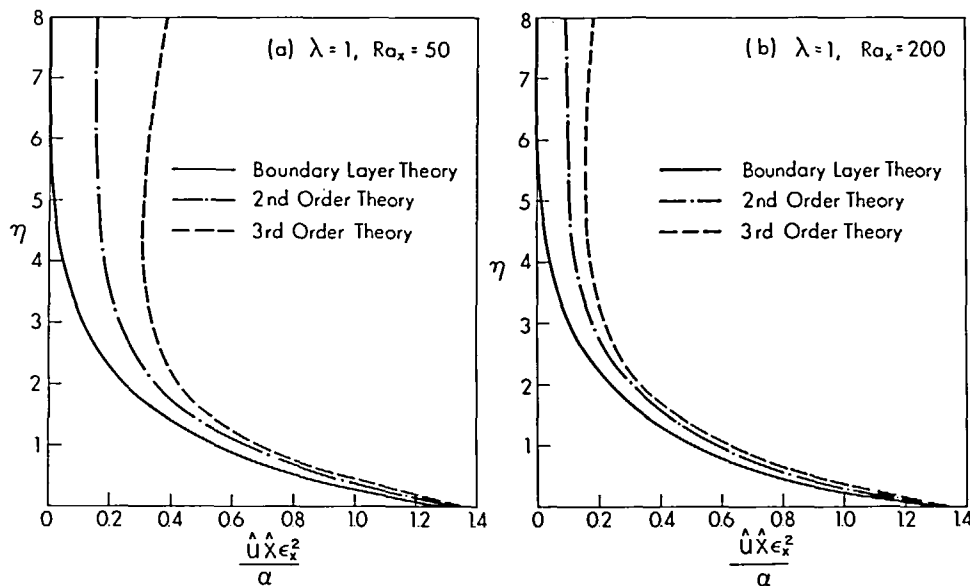


FIG. 10. Dimensionless horizontal velocity profiles for  $\lambda = 1$ : (a)  $Ra_x = 50$  and (b)  $Ra_x = 200$ .

obtained from the second-order theory in this figure are positive rather than negative as in Fig. 9.

Higher-order corrections to temperature and heat flux. With the aid of equations (32b), (52b), (66b) and (16b), the inner expansion for temperature is

$$\begin{aligned}
 (\hat{T} - \hat{T}_\infty)/(\hat{T}_w - \hat{T}_\infty) &= g_0(\eta) - \epsilon_x [(\lambda + 1)/3] \cot[\pi(\lambda + 1)/3] \\
 &\times f_0(\infty)g_1(\eta) + \epsilon_x^2 g_2(\eta) + O(\epsilon_x^3) \quad (0.1 \leq \lambda < 2) \quad (100)
 \end{aligned}$$

which is plotted in Figs. 11(a) and 11(b) for  $Ra_x = 50$  with  $\lambda = 0.1$  and  $\lambda = 1$  respectively. It is shown that all higher-order corrections in temperature are small even at small value of Rayleigh number.

The Nusselt number  $Nu_x = h\bar{x}/k$  can be obtained from the differentiation of equation (100) which yields

$$\begin{aligned}
 Nu_x/(Ra_x^{1/3}) &= -\{g'_0(0) - \epsilon_x [(\lambda + 1)/3] \\
 &\times f_0(\infty) \cot[\pi(\lambda + 1)/3] g'_1(0) \\
 &+ \epsilon_x^2 g'_2(0) + O(\epsilon_x^3)\}. \quad (101)
 \end{aligned}$$

Equation (101) was computed for various local Rayleigh numbers and  $\lambda$ , and the results are given in

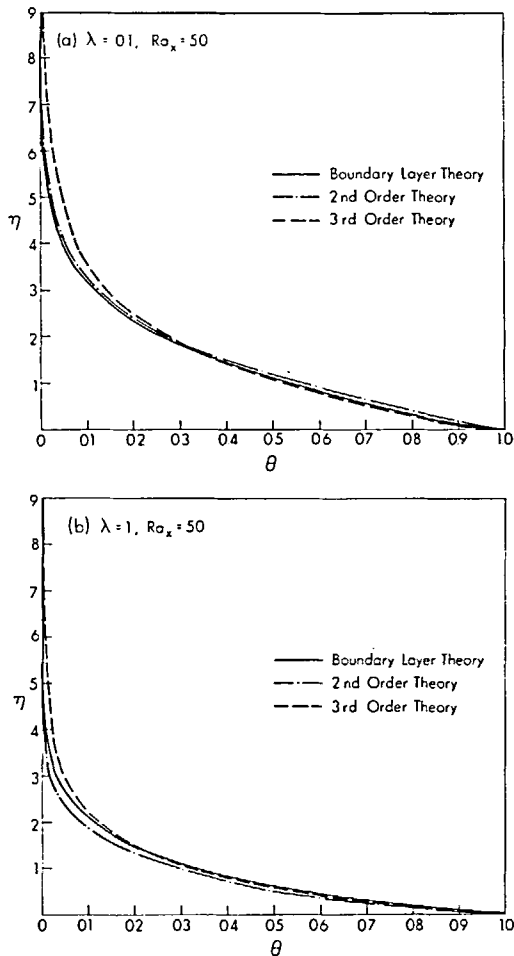


FIG. 11. Dimensionless temperature profiles at  $Ra_x = 50$ : (a)  $\lambda = 0.1$  and (b)  $\lambda = 1$ .

Table 2. Local Nusselt numbers versus local Rayleigh numbers at selected values of  $\lambda$

$Ra_x$	$\lambda = 0$			$\lambda = 0.1$			$\lambda = 0.5$			$\lambda = 1.0$			$\lambda = 1.5$		
	1st approx.	2nd approx.	3rd approx.	1st approx.	2nd approx.	3rd approx.	1st approx.	2nd approx.	3rd approx.	1st approx.	2nd approx.	3rd approx.	1st approx.	2nd approx.	3rd approx.
30	1.334	1.334	—	1.633	1.586	1.660	2.536	2.536	2.536	3.411	3.659	3.586	4.179	5.060	4.756
50	1.582	1.582	—	1.937	1.890	1.952	3.007	3.007	3.007	4.045	4.293	4.232	4.954	5.836	5.580
100	1.994	1.994	—	2.440	2.394	2.443	3.789	3.789	3.789	5.096	5.346	5.297	6.242	7.125	6.922
200	2.512	2.512	—	3.074	3.029	3.068	4.774	4.774	4.774	6.421	6.673	6.634	7.865	8.748	8.587
500	3.412	3.412	—	4.173	4.128	4.157	6.480	6.480	6.480	8.722	8.970	8.941	10.67	11.56	11.44

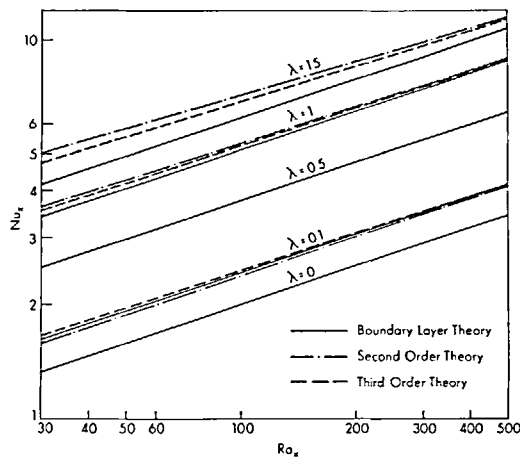


FIG. 12. Local Nusselt numbers versus local Rayleigh numbers for selected values of  $\lambda$ .

Table 2 for future reference. It is noted from the table that for the case of  $\lambda = 0$ , the first (boundary layer) and second-order theories give identical results for the local Nusselt number because of the fact that  $g_1 = g'_1 = 0$ . For the case of  $\lambda = 0.5$ , all three theories give identical results for the local Nusselt number because  $\cot[\pi/2] = 0$  and  $g'_2(0) = 0$ . For other values of  $\lambda$ , the value of  $Nu_x$  obtained from the *second-order* theory may be higher than or lower than the boundary layer theory depending on whether  $\lambda > 0.5$  or  $\lambda < 0.5$ , because the second term in equation (101) changes signs at  $\lambda = 0.5$ . On the other hand, the value of  $Nu_x$  obtained from the *third-order* theory is always higher than the boundary layer theory. A comparison of Nusselt numbers obtained from the first, second and third-order theory is present in Fig. 13, which shows that the boundary layer theory is quite accurate even for moderate values of Rayleigh number; the accuracy of the boundary layer theory decreases as the Rayleigh number is decreased, and as  $\lambda$  is increased from  $\lambda = 1$ .

### 3. CONCLUSIONS

The following general conclusions can be drawn from the analysis:

(1) There are in general three effects contained in the higher order approximations, namely, fluid entrainment, upward-drift-induced frictional force, and streamwise heat conduction. The resultant effects are a slight increase in the slope of the temperature profile near the wall (with a corresponding increase in surface heat flux) and a modification of the velocity near the edge of the boundary layer where the velocity of the inner flow matches with those of the outer flow.

(2) The temperature perturbation inside the boundary layer decays exponentially toward the outer edge of the layer. There is no heat transfer between the boundary layer and the region outside the boundary layer. An isothermal fluid motion is induced, however, in the outer region.

(3) The sole interaction between the boundary layer and the outside region is by way of fluid entrainment. The entrainment is from the outside into inside the boundary layer along the edge of the boundary layer.

(4) The temperature distribution inside the boundary layer is modified by the convection of the entrainment induced flow in the second and third-order theory, as well as by the streamwise heat conduction in the third-order theory.

(5) The higher-order theory has a larger effect on velocity profiles and a smaller effect on temperature profiles.

(6) The local Nusselt numbers as obtained from the boundary layer theory for  $\lambda = 0.5$  are accurate to the third-order while those for  $\lambda = 0$  are accurate to the second-order. For other values of  $\lambda$ , the boundary layer theory also gives accurate results for the local Nusselt numbers even at moderate values of Rayleigh numbers. The accuracy of the boundary layer theory decreases as the Rayleigh numbers decrease and as  $\lambda$  increases from  $\lambda = 0.5$ .

*Acknowledgements*—This work was supported by the National Science Foundation through Grants No. ENG 77-27527 and MEA 81-00437. The authors wish to thank Dr C. T. Hsu for pointing out an error in the third-order theory and for helpful discussion on eigenfunctions. They would also like to thank M. Karmarkar, C. L. Chan, and T. T. Luc for their assistance in the numerical computations.

### REFERENCES

1. P. Cheng and I-Dee Chang, Buoyance induced flows in a saturated porous medium adjacent to impermeable horizontal surfaces, *Int. J. Heat Mass Transfer* **19**, 1267–1272 (1976).
2. M. Van Dyke, *Perturbation Methods in Fluid Mechanics*. Academic Press, New York (1964).
3. K. T. Yang and E. W. Jerger, First order perturbations of laminar free-convection boundary layers on a vertical plate, *J. Heat Transfer* **86**, 107–115 (1964).
4. C. A. Hieber, Natural convection around a semi-infinite vertical plate: Higher-order effects, *Int. J. Heat Mass Transfer* **17**, 785–791 (1975).
5. R. L. Mahajan and B. Gebhart, Higher order approximations to the natural convection flow over a uniform flux vertical surface, *Int. J. Heat Mass Transfer* **21**, 549–556 (1978).
6. R. L. Mahajan and B. Gebhart, Higher-order boundary layer effects in plane horizontal natural convection flows, *J. Heat Transfer* **102**, 368–371 (1980).
7. P. Cheng, Heat transfer in geothermal systems, in *Advances in Heat Transfer*, Vol. 14, pp. 1–105. Academic Press, New York (1978).

DEVELOPPEMENTS ASYMPTOTIQUES POUR LA CONVECTION NATURELLE PRES  
D'UNE SURFACE HORIZONTALE ET IMPERMEABLE DANS UN MILIEU POREUX

Résumé— Le problème de la convection naturelle stationnaire dans un milieu poreux adjacent à une surface chaude, horizontale et imperméable, avec une distribution de température pariétale  $\hat{T}_w = \hat{T}_\infty + A\hat{x}^\lambda$  pour  $\hat{x} > 0$  et  $\hat{T}_w = \hat{T}_\infty$  à  $\hat{x} < 0$  ( $0 < \lambda < 2$ ), est étudié par la méthode des développements asymptotiques. Le petit paramètre dans les séries de perturbation est l'inverse de la puissance un tiers du nombre de Rayleigh. Pour le premier ordre du problème interne, les équations de base se réduisent aux approximations de la couche limite qui a déjà été résolue par les auteurs. Les effets de l'entraînement du fluide, de la conduction thermique et du frottement induit sont pris en considération dans la théorie du second et du troisième ordre pour laquelle on obtient les solutions de similarité. On présente les résultats numériques pour les profils de température et de vitesse et pour le nombre de Nusselt local à différents nombres de Rayleigh locaux et différentes distributions de température pariétales données. On trouve que les nombres de Nusselt locaux obtenus par la théorie de la couche limite pour  $\lambda = 0,5$  sont précis jusqu'au troisième ordre, tandis que ceux pour  $\lambda = 0$  sont précis au second ordre. Pour d'autres valeurs de  $\lambda$ , la théorie de couche limite sous-estime légèrement le nombre de Nusselt local; la précision de la théorie de couche limite décroît lorsque le nombre de Rayleigh diminue et lorsque  $\lambda$  croît au dessus de 0,5.

ANGEPASSTE ASYMPTOTISCHE ENTWICKLUNGEN FÜR DIE FREIE KONVEKTION  
ÜBER EINER UN DURCHLÄSSIGEN WAAGERECHTEN OBERFLÄCHE IN EINEM  
PORÖSEN MEDIUM

Zusammenfassung— Der Mechanismus der stationären freien Konvektion in einem porösen Medium über einer waagerechten undurchlässigen Heizfläche mit der Temperaturverteilung  $\hat{T}_w = \hat{T}_\infty + A\hat{x}^\lambda$  ( $0 \leq \lambda < 2$ ) für  $\hat{x} \geq 0$  und  $\hat{T}_w = \hat{T}_\infty$  für  $\hat{x} < 0$  wird mit Hilfe der Methode der angepaßten asymptotischen Entwicklungen untersucht. Es wurde herausgefunden, daß der kleine Parameter in den Störungsreihen umgekehrt proportional der Rayleigh-Zahl hoch ein Drittel ist. Für das innere Problem erster Ordnung sind die kennzeichnenden Gleichungen auf die Grenzschichtnäherungen zurückgeführt, die kürzlich von denselben Autoren gelöst wurden.

Die Einflüsse des Entrainments, der Wärmeleitung in Strömungsrichtung und der durch die Aufwärtsdrift hervorgerufenen Reibung werden in der Theorie zweiter und dritter Ordnung berücksichtigt, für die sich Ähnlichkeitslösungen ergeben. Für das Temperatur- und Geschwindigkeitsprofil in Strömungsrichtung werden numerische Ergebnisse vorgestellt, ebenso für die örtliche Nußeltzahl bei verschiedenen örtlichen Rayleigh-Zahlen und unterschiedlichen aufgeprägten Wandtemperaturverteilungen. Es zeigt sich, daß die mit der Grenzschichttheorie für  $\lambda = 0,5$  erhaltenen örtlichen Nußeltzahlen mit denen der dritten Ordnung übereinstimmen, während diejenigen für  $\lambda = 0$  mit denen der zweiten Ordnung übereinstimmen. Für andere Werte von  $\lambda$  ergibt die Grenzschichttheorie geringfügig zu kleine örtliche Nußelt-Zahlen; die Genauigkeit der Grenzschichttheorie nimmt in dem Maß ab, wie die Rayleigh-Zahl kleiner und wie  $\lambda$  von  $\lambda = 0,5$  an größer wird.

СРАЩИВАЕМЫЕ АСИМПТОТИЧЕСКИЕ РАЗЛОЖЕНИЯ ДЛЯ СВОБОДНОЙ  
КОНВЕКЦИИ У НЕПРОНИЦАЕМОЙ ГОРИЗОНТАЛЬНОЙ ПОВЕРХНОСТИ  
В ПОРИСТОЙ СРЕДЕ

Аннотация— Задача стационарной свободной конвекции в пористой среде у горизонтальной непроницаемой нагреваемой поверхности, характеризующейся распределением температур  $\hat{T}_w = \hat{T}_\infty + A\hat{x}^\lambda$  ( $0 \leq \lambda < 2$ ) при  $\hat{x} \geq 0$  и  $\hat{T}_w = \hat{T}_\infty$  при  $\hat{x} < 0$ , исследуется методом сращиваемых асимптотических разложений. Найдено, что малый параметр равен обратному числу Рэлея в степени  $1/3$ . Для внутренней задачи первого порядка основные уравнения сводятся к приближениям пограничного слоя, которые решены авторами ранее. Увлечение жидкости, теплопередача по направлению течения и трение, вызванное направленным вверх дрейфом, учитываются зависимостями второго и третьего порядка, для которых получены автомодельные решения. Представлены численные результаты по профилям температур и скорости по направлению течения, а также локальному числу Нуссельта при различных значениях локального числа Рэлея и различных заданных распределениях температур стенки. Найдено, что значения локального числа Нуссельта, полученные из теории пограничного слоя, являются точными до третьего порядка при  $\lambda = 0,5$  и до второго порядка при  $\lambda = 0$ . При других значениях  $\lambda$  получаются несколько заниженные значения локального числа Нуссельта; точность теории пограничного слоя уменьшается по мере уменьшения числа Рэлея и увеличения  $\lambda$  выше 0,5.